

DEVELOPMENT OF OVERSTRENGTH FACTORS FOR MULTI-PANEL CLT SHEAR WALLS BASED ON PANEL-TO-PANEL CONNECTIONS

Antoine Bérubé¹, Ghasan Doudak²

ABSTRACT: This paper presents the results of an ongoing study aimed at developing overstrength factors for the design of multi-panel platform-type CLT shear walls. A hierarchy of failure has been introduced in the new edition of the Canadian Engineering Design in Wood (CSA O86) standard, in which dissipative and non-dissipative components are required to be designed based on the strength variation of the panel-to-panel vertical joint connections. Experimental results from cyclic tests on spline panel-to-panel joints are presented, and the framework used to extract overstrength factors from the test results is discussed. The results indicate that an overstrength factor due to connection strength variability of approximately 1.3 is adequate to modify the 5th percentile of the connection strength to the 95th percentile level. However, the results also show that the analytical overstrength factor, i.e., that reflecting the difference between the 5th percentile strength and the design capacity obtained from the Canadian timber design standard is relatively much higher, especially for screw connections at large displacements.

KEYWORDS: capacity-based design, overstrength factor, cross-laminated timber (CLT), panel-to-panel connection

1 – INTRODUCTION

The newly published edition of the Canadian Engineering Design in Wood (CSA O86 [1]) standard includes a procedure outlining the sequence of failure amongst various CLT shear wall connections in multi-panel platform-type CLT buildings, in order to ensure adequate energy dissipation, especially in seismic-prone regions. In this prescribed hierarchy, the first component required to yield is the panel-to-panel connection (i.e., vertical joint) due to its ability to provide significantly more energy dissipation than the other components (e.g., hold-downs and angle brackets) when the kinematic mode is coupled-wall behaviour (e.g., [2–4]). The yielding of the panel-to-panel joints is followed by the yielding and eventual failure of the hold-down, angle brackets, and then CLT panels. The standard also contains a design procedure that relates the resistance of all the components that are not the primary energy dissipative elements to that of the panel-to-panel connections through a factor, which can be determined based on the distribution of strength properties in the panel-to-panel connection. As such, non-dissipative (i.e., CLT and angle brackets) and other dissipative (i.e., hold-downs) components are required to remain elastic when the panel-to-panel connections reach a given percentile of their resistance, corresponding to the 95th percentile

for the CLT panel, and 30th and 15th percentile for the angle brackets and hold-down, respectively. This paper presents the results of an on-going experimental campaign with the aim to provide an estimate for overstrength factors for commonly used panel-to-panel connectors (e.g., nails and screws), and proposes procedures for how such overstrength factors can be estimated.

2 – BACKGROUND

2.1 PERFORMANCE OF CLT SHEAR WALLS

Several studies have investigated the behaviour of CLT shear walls through full-scale testing at the wall level [5–7] and the use of a shake table on entire structural systems [8,9]. The panel-to-panel and wall-to-floor connections were identified as a key contributor to the lateral performance of CLT shear walls [10]. The SOFIE project included an experimental investigation of a full-scale 3- and 7-storey buildings on a shake table [9,11] as well as on individual walls [12] and indicated that properly designed CLT buildings could withstand severe earthquakes. CLT panels were observed to remain almost rigid during testing, with damage and deformation concentrated in the connections [5,13]. Wall-level tests indicated that ductility was much greater when rocking

¹ Antoine Bérubé, PhD Student, Department of Civil Engineering, University of Ottawa, Ottawa, Canada, aberu025@uottawa.ca.

² Ghasan Doudak, Professor, Department of Civil Engineering, University of Ottawa, Ottawa, Canada, gdoudak@uottawa.ca

behaviour dominates [7,14,15], which is more likely to occur when walls consist of multiple panels [13].

Studies found that vertical load [5,13] and hold-down devices [13] provided beneficial effects on the performance of CLT shear walls, while the cyclic nature of the loading diminishes the performance compared to static (monotonic) loading by observing reduced peak load and displacement capacity [13,16]. This can be partially attributed to the low cycle fatigue of fasteners, a phenomenon that has been observed to be significant in small-diameter fasteners [13].

Three kinematic deformation mechanisms identified in the established literature (i.e. [3,17]) include: a) coupled-panel behaviour (CP), b) intermediate behaviour (IN), and c) single wall behaviour (SW). CP behaviour occurs when the individual panels rock about their respective point of rotation. To achieve this mechanism, the vertical joints must generally be relatively weaker and softer than the hold-downs. SW behaviour occurs when the entire wall rocks about a single point, where the vertical joints are stiffer and stronger than the hold-down connections. IN behaviour is an intermediate case between the previous two mechanisms, where some of the wall panels behave in CP and others in SW. CP is the preferred behaviour, particularly in high seismic-prone areas, since the deformation experienced in the panel-to-panel connections provides significant ductility. It is thus important that panel-to-panel connections are prioritized in the yielding hierarchy and that all other components are capacity-protected to varying degrees.

Ductile failure in panel-to-panel connections depends on the formation of plastic hinges in the fasteners used to connect the CLT panels [18–20]. Spline joints with screws installed at 90 degrees have been observed to be more ductile and less stiff than those at an angle [21]. While angled screwed connections can be stiffer, they do not promote the formation of plastic hinges [18,22]. Low-cycle fatigue in panel-to-panel connections has been observed in several studies (e.g., [21,23,24]).

2.2 CAPACITY DESIGN PHILOSOPHY

Ductility is crucial for adequate performance of any structure under extreme loading events such as earthquakes since it allows forces to be redistributed between elements and energy to be dissipated through plastic deformation. Promoting ductile mechanisms can delay or prevent brittle failure modes that cause sudden and severe failures (e.g., splitting). Jorissen and Fragiaco [25] developed a procedure to protect brittle timber elements through a capacity-based design philosophy. Since timber structures rely on connections

to achieve ductility, the brittle timber elements are usually protected, while ductile elements (i.e., connections) are allowed to yield to attain energy dissipation. The statistical distribution on the strength of all components must be characterized to promote a proper hierarchy of failure through the design of components. In the case of CLT shear walls, components like panel-to-panel joints, hold-downs, and angle brackets possess varying degrees of ductility. To obtain adequate energy dissipation, the hierarchy of failure necessitates yielding in the vertical joints followed by the hold-downs, angle brackets and then the CLT panels [3,17]. It is also required that the vertical joint failure mode is one that develops one- or two plastic hinges in the fastener (i.e., mode d, e, or g in CSA O86 [1]). As proposed by Jorissen and Fragiaco [25], the overstrength factor can be calculated according to (1):

$$\gamma_{Xth} = \gamma_{sc,Xth} \gamma_{an} = \left(\frac{R_{Xth}}{R_{5th}} \right) \left(\frac{R_{5th}}{R_D} \right) \quad (1)$$

Where $\gamma_{sc,Xth}$ is the overstrength factor resulting from the strength distribution in the connection between the Xth and 5th percentiles (R_{Xth} and R_{5th}), which can be extracted from test results, and γ_{an} is the overstrength factor resulting from the difference between the 5th percentile strength and the design capacity (R_D), with the latter obtained from standards such as CSA O86 [1]. This paper will provide examples and discussion based on overstrength factors at the 95th percentile only, which is representative of non-dissipative components in CSA O86 [1].

3 – EXPERIMENTAL PROGRAM

3.2 NUMBER OF REPLICATES

The development of overstrength factors requires knowledge of the statistical distribution of the resistance in panel-to-panel connections. The number of tested replicates in the current study was based on analysis following ASTM D2915-17 [26] in order to ensure that the number of replicates would allow for near-minimum properties (i.e., 5th and 95th percentiles) to be predicted with a 75% confidence interval and 5% estimate of precision. In this analysis, the coefficient of variation (CoV) was selected based on similar testing of spline joints available in the literature (e.g., [4,19,21]). This analysis resulted in the selection of 10 replicates for cyclic testing. Three additional replicates were also selected for monotonic testing, which is required to generate the cyclic testing protocol.

3.3 SPECIMEN DESCRIPTION AND TEST MATRIX

The vertical joint specimens comprised 3-ply (105 mm thick) CLT panels of grade E1 obtained from Nordic Structures (QC, Canada) and 25.4 mm (1 in.) Douglas Fir plywood (DFP) obtained from a local hardware store. Figure 1 shows the CLT specimen's geometry, consisting of two side pieces and one centre piece to avoid eccentricity during testing. Gaps were provided between the sides of the plywood spline and the CLT pieces to reduce friction during testing.

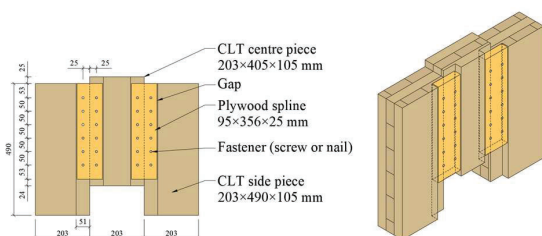


Figure 1: Geometry of spline joint specimens

Screws and nails are commonly used in vertical joints and have both been considered in the development of the test matrix. Fastener size, particularly diameter, can significantly impact the performance of the joint and the potential for low-cycle fatigue. Partially threaded self-tapping screws with nominal diameters of 6 mm and 8 mm and length of 100 mm were selected. For nails, 16d smooth shank common bright nails were also chosen. Table 1 summarizes the specimen configurations.

Table 1: Specimen configurations

Configuration	Fastener type	Size	Average $\Delta_{u,m}$ (mm)
N-16d	Common nail (N) Smooth shank	16d (4.2×88.9 mm)	49.3
S-6×100	Self-tapping screw (S)	6×100 mm	65.3
S-8×100	Partially threaded	8×100 mm	56.9

Six fasteners per row were chosen to provide a reasonable representation of the vertical joints. A spacing of 50.8 mm (2 in.) between each fastener was used, which met the requirements of CSA O86 [1]. Furthermore, ductile governing failure mode, which includes plastic hinge formation, was verified according to CSA O86 [1].

3.2 TEST SET UP AND PROTOCOL

The test setup for the joint tests is illustrated in Figure 2a with a picture of a specimen presented in Figure 2b. The displacement in the joint was induced by clamping the side pieces to remain stationary while affixing the centre piece to the Universal Testing Machine (UTM) actuator using a reinforced steel plate, allowing the reverse cyclic

movement of the centre piece in the vertical direction. The centre piece was similarly clamped using a top plate (attached to the UTM's actuator) and a bottom plate connected with tightened threaded rods. Additional steel pieces and threaded rods were added horizontally as lateral support to avoid opening in the specimens and separation between the CLT pieces. It was ensured that this connection was only hand-tightened to avoid unwanted wedging or friction, which could potentially affect the results. Two string potentiometers were used to measure the slip in the joint, while loading was recorded using a load cell. Loading was normalized to represent a single fastener at standard-term loading.

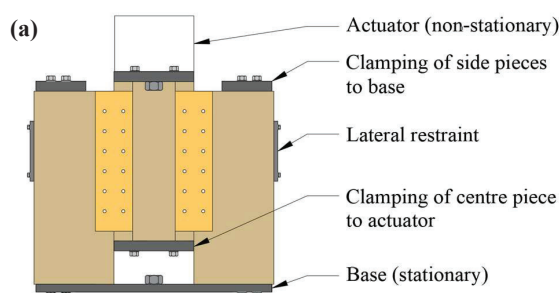


Figure 2: a) Illustration of test setup; and b) Picture of test specimen

Method B of ASTM E2126 [27] (based on ISO 16670 [28]) was selected as the displacement-controlled test protocol for cyclic testing. The protocol follows a fully reversed repeating pattern with increasing amplitudes defined in terms of the monotonic ultimate displacement ($\Delta_{u,m}$), identified as the displacement at which there is a 20% reduction in load following the peak (or 80% of the peak load). For monotonic testing, a displacement-controlled protocol at a 10 mm/min (0.167 mm/s) rate was used (ASTM E2126 [27] requires less than 25 mm/min). The average monotonic ultimate displacement used to generate the cyclic protocol for each series is presented in Table 1. A 60 mm/min (1 mm/sec) displacement rate was selected for cyclic testing, which is the minimum required rate from Method B of ASTM E2126 [27] (1 mm/s to 63.5 mm/s). Given the loading

rate and the repeating cyclic protocol, tests were anticipated to be completed in less than 30 minutes, which is appropriate for testing wood elements to avoid creep effects. Compression and tension in the cyclic tests were assumed to be positive and negative, respectively.

4 – RESULTS

4.1 CYCLIC TEST RESULTS

Figure 3 presents the cyclic load-displacement results for the three test series, where the first replicate of each series is highlighted in black, while all other replicates of the same series are presented in grey in the background. It can be observed that each series shows small variations between the 10 replicates, especially prior to reaching the peak load. Low-cycle fatigue was observed to be more prevalent in connections with 6 mm diameter screws (Figure 3b) than those with 8 mm diameter (Figure 3c), while nails experienced little to no low-cycle fatigue (i.e., Figure 3a).

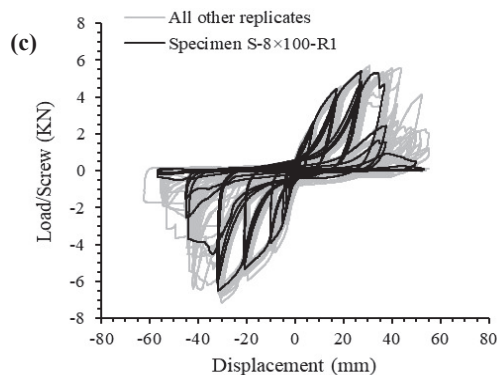
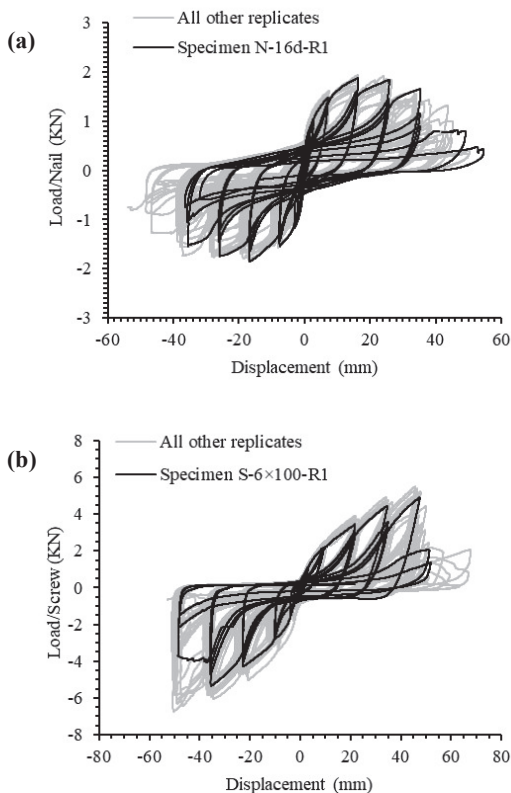
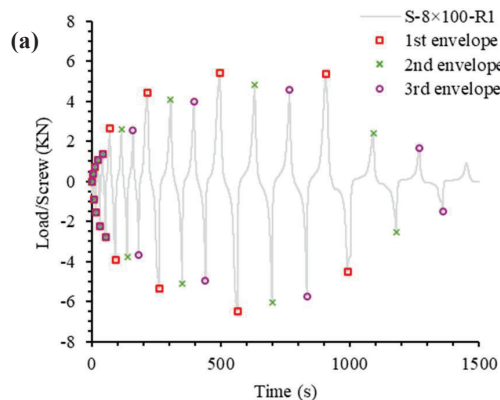


Figure 3: Cyclic test results for a) 16d nails (N-16d), b) 6x100 mm screws (S-6x100), and c) 8x100 mm screws (S-8x100)

4.2 CYCLIC ENVELOPE CURVES

The first step in developing the overstrength factor values based on the cyclic test results is to obtain the individual cyclic envelope curves for each replicate by connecting the load peaks in the cyclic load-displacement relationship (Figure 4a), for the first, second, and third cycles, respectively (Figure 4b). Since the positive and negative (reversed) envelope curves were within 20% variation, reasonable symmetry was assumed and an average envelope curve was used for each replicate (i.e., Figure 4c). The resulting averaged envelope curves for all test series and replicates are presented in Figure 6. The strength degradation between cycles is obtained by the ratio of the peaks for the respective cycles.



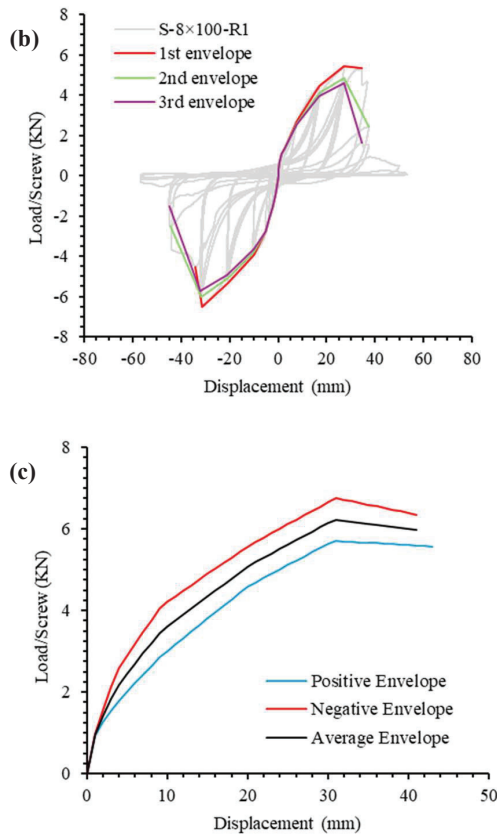


Figure 4: Examples of a) load peaks in load-time history, b) obtaining the cyclic envelopes from the load peaks, and c) averaging of positive and negative envelopes

4.3 MECHANICAL PARAMETERS

Mechanical parameters were extracted from the averaged cyclic first envelope curves, including peak load (F_{max}) and corresponding peak displacement (Δ_{max}). The elastic stiffness (K_e) was calculated using the points on the envelope curves corresponding to load values of $0.1F_{max}$ and $0.4F_{max}$. As recommended by the ASTM E2126-19 [27] and EN12512 [29] standards, a 20% reduction in the load resistance following the peak (equivalent to $0.8F_{max}$) is considered to result in the failure of the connection. However, this interpretation does not consider strength degradation between repetitive cycles at the same displacement, as with the cyclic protocol employed in this study. As such, an additional criterion based on the strength impairment in EN12512 [29] was considered for the ultimate point, where a strength degradation from the 1st to the 3rd envelope of 30% or more was also considered to result in failure. Thus, the ultimate displacement (Δ_u) was taken as the minimum displacement between the two criteria with corresponding ultimate load (F_u). This provides a more conservative prediction of the ultimate displacement and

ductility. The yield point, defined by the yield displacement and load, was calculated using both the EEEP method from ASTM E2126-19 [27] ($\Delta_{y,EP}$, $F_{y,EP}$) and the method presented in the EN12512 standard [29] ($\Delta_{y,EN}$, $F_{y,EN}$). The EEEP method defines the yield displacement and load according to (2) and (3), respectively, which depend on the area (A) under the envelope curve representing energy dissipation. The EN12512 [29] method defines the yield point as the intersection of two lines. The first line is the initial linear-elastic portion with slope K_e , which passes through the origin. The second line has a slope equal to $K_e/6$, which is tangent to the cyclic envelope. Figure 5 presents a typical example of obtaining the yield point from the EEEP and EN12512 methods, with the yield point of both methods being indicated with a dot. Since both methods provide different yield point estimates, they will also result in different ductility ratios ($\mu_{u,EP}$ and $\mu_{u,EN}$). Other methods to estimate the yield point, such as the 5% offset method, are not presented in this paper. Table 2 summarizes the average and associated CoVs of the mechanical parameters mentioned above for each series.

$$\Delta_{y,EP} = \Delta_u - \sqrt{\Delta_u^2 - 2A/K_e} \quad (2)$$

$$F_{y,EP} = \Delta_{y,EP}K_e \quad (3)$$

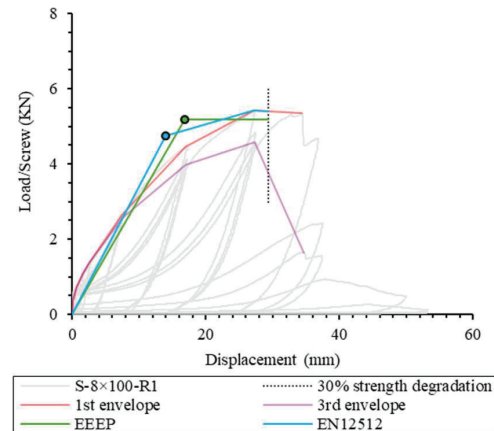


Figure 5: Typical example of obtaining the yield point from the EEEP and EN12512 methodologies

Table 2: Average and CoV for mechanical parameters extracted from the averaged cyclic envelopes for 10 replicates

Mechanical Parameter	N-16d		S-6×100		S-8×100	
	Average	CoV (%)	Average	CoV (%)	Average	CoV (%)
K_e (kN/mm/fastener)	0.86	60.5	0.26	7.9	0.43	10.2
Δ_{max} (mm)	18.9	24.2	43.5	8.7	30.5	5.8
F_{max} (kN/fastener)	1.72	7.1	5.49	6.1	6.05	2.8
$\Delta_{y,EP}$ (mm)	2.9	20.2	18.2	10.2	13.8	7.7
$F_{y,EP}$ (kN/fastener)	1.54	7.4	4.56	6.5	5.31	4.7
$H_{y,EP}$ (°)	16.0	63.8	2.1	9.1	2.8	14.5
$\Delta_{y,EN}$ (mm)	1.9	27.9	16.5	10.8	11.3	8.7
$F_{y,EN}$ (kN/fastener)	0.98	6.5	4.40	5.9	4.59	6.1
$H_{y,EN}$ (°)	31.9	66.7	2.4	10.1	3.6	21.8
Δ_u (mm)	28.8	12.2	38.1	3.9	34.1	9.6
F_u (kN/fastener)	1.53	8.8	5.17	6.1	5.46	6.7

4.4 STRENGTH DISTRIBUTION OVERSTRENGTH FACTOR

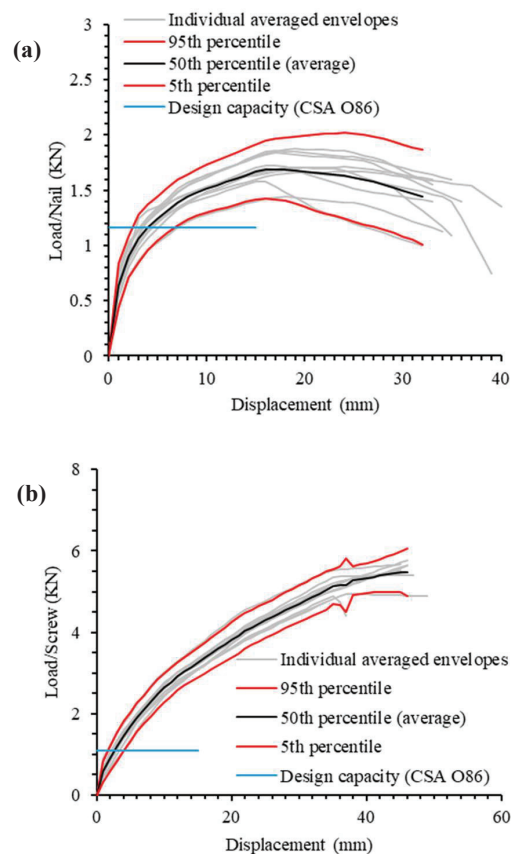
Obtaining the overstrength factor requires extracting the 5th and 95th percentiles from the individual averaged envelope curves based on (4), which assumes normal distribution.

$$R_{Xt} = R_{avg}(1 + K_{Xth} \times CoV) \quad (4)$$

Where R_{Xth} is the resistance at the X^{th} percentile, R_{avg} is the average resistance of the 10 replicates, K_{Xth} is a constant to bring the values from the average to the X^{th} percentile, and CoV is the coefficient of variation for the 10 replicates. K_{Xth} depends on the confidence interval (75%), the percentile (e.g., 95th), and the number of tests (10) and was calculated according to the equations developed by Link [30] as recommended in ASTM D2915-17 [26]. For 10 replicates, K_{Xth} was calculated to be -2.1 and 2.1 at the 5th and 95th percentiles, respectively.

The 5th and 95th percentiles can be calculated based on load values on the load-displacement curve at a given point or displacement level, the definition of which is not always explicitly stated. Different results could be obtained depending on how one selects values to calculate the 5th and 95th percentiles. In order to investigate this, multiple methodologies were considered for the screw connections, including a) using the peak load (F_{max}), b) using the load values at a given displacement level, and c) using the yield load. The different methodologies will result in varying overstrength factors for the connection strength

distribution ($\gamma_{sc,95th}$), which only depends on test results. Using F_{max} provides a simple way to extract the overstrength factor but does not allow a set definition of the displacement level since the displacement associated with F_{max} varies between tests. Using the load values at a set displacement level allows the overstrength factor to be linked to other criteria (e.g., drift limits, acceptance criteria, etc.). Figure 6 shows the 5th and 95th percentile values plotted in the same graphs as those obtained from the experimental tests. Some standards provide guidance on which displacement value could be used. Examples include 15 mm (EN26891 [31]) and 30 mm (EN12512 [29]), but lower displacement values such as 5 mm could also be of interest since design values are usually based on elastic design at much lower displacements than those observed under seismic loading.



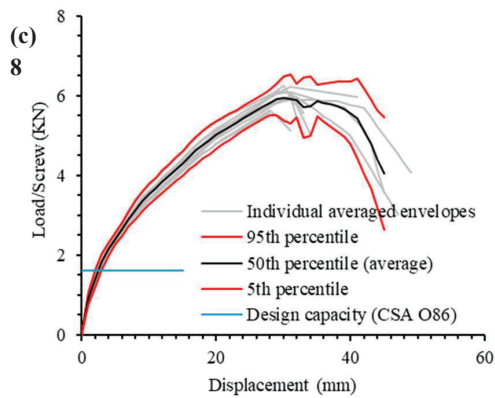


Figure 6: Obtaining the 5th and 95th percentiles based on the individual averaged envelopes and comparison with design capacity from CSA O86 for series a) N-16d, b) S-6×100, and c) S-8×100

Table 3 presents the 5th percentile, 95th percentile, and resulting overstrength factors for strength distribution ($\gamma_{sc,95th} = R_{95th}/R_{5th}$) for the three series of ten replicates and methodologies presented above. From the $\gamma_{sc,95th}$ values presented in Table 3, it can be observed that this factor does not vary significantly between series and methodology employed, with an average value equal to 1.3.

4.5 ANALYTICAL OVERSTRENGTH FACTOR

The analytical overstrength factor ($\gamma_{an} = R_{5th}/R_D$) depends on the 5th percentile value extracted from the test results and the design capacity obtained from the relevant standard. As such, a panel-to-panel connection will not have a universally applicable value (across various design standards) of γ_{an} even though the connection has the same 5th percentile value. The uncertainty in selecting a 5th percentile value associated with a given displacement (or load) stems from the fact that the majority of timber design standards have adopted the European Yield Model (EYM), for which inputs include the yield strength (or moment) of the fastener and the embedment strength of the wood element. This yield strength cannot be associated with a given displacement in a specific connection, which makes the choice of displacement-related strength level from the test results ambiguous.

The value for γ_{an} obtained based on the CSA O86 [1] standard design approach is used as an example to demonstrate the procedure. According to the CSA O86 provisions, values of 1.16 kN/nail, 1.09 kN/screw, and 1.62 kN/screw were obtained for design capacity (R_D) of series N-16d, S-6×100, and S-8×100, respectively. As can be observed in Figure 6, the design capacity from

CSA O86 [1] is reached in the 5th percentile of the test results at values of 6.7 mm, 4.0 mm, and 3.0 mm for series N-16d, S-6×100, and S-8×100, respectively. Table 3 presents the resulting values of γ_{an} for the various methodologies to obtain the 5th percentile, as presented previously.

Table 3: 5th and 95th percentiles and resulting overstrength factors on connection strength distribution

Series	Methodology	R_{5th} (kN/fastener)	R_{95th} (kN/fastener)	$\gamma_{sc,95th}$ ()	γ_{an} ()	γ ()
N-16d	Peak	1.46	1.98	1.35	1.26	1.70
S-6×100	Peak	4.79	6.19	1.29	4.40	5.68
	5 mm	1.33	2.05	1.54	1.22	1.88
	15 mm	2.90	3.62	1.25	2.65	3.32
	30 mm	4.26	5.14	1.21	3.90	4.72
	EEEEP yield	3.94	5.18	1.32	3.61	4.75
	EN12512 yield	3.85	4.95	1.28	3.53	4.54
S-8×100	Peak	5.69	6.41	1.13	3.51	3.96
	5 mm	2.27	2.55	1.12	1.36	1.53
	15 mm	4.00	4.62	1.15	2.40	2.77
	30 mm	5.39	6.49	1.20	3.23	3.89
	EEEEP yield	4.79	5.83	1.22	2.87	3.49
	EN12512 yield	4.00	5.18	1.29	2.40	3.11

4.6 PRACTICAL CONSIDERATIONS AND FINAL OVERSTRENGTH FACTOR

There is a practical limitation to what can be selected as overstrength factor to be implemented in a design standard. For example, the NBCC [32] allows an $R_d R_o$ factor equal to 1.3 to be the lower limit in design, resulting in an upper limit on the base shear (V_e) equal to $0.77V_e$ as demonstrated in Equation 5. For the case of a design based on a moderately ductile timber load-resisting system, the NBCC [32] allows for an R_d and R_o factor values of 2.0 and 1.5, respectively, which means that non-dissipative components must be designed to a base shear load equal to $0.33 \gamma_{95th} V_e$, as demonstrated in Equation 6. Thus, if the overstrength factor value (γ_{95th}) is greater than 2.31 (as demonstrated in Equation 7), then elastic design would govern. As can be observed from Table 3, γ_{95th} is less than 2.31 for the nailed connection at the peak. However, for screw connections, only the 5 mm displacement-level results in γ_{95th} values that are less than 2.31. It is encouraged that the scientific community reach a consensus on some of the ambiguity raised in this paper such that consistency in design and safety can be achieved.

$$\frac{V_e}{R_d R_o} = \frac{V_e}{(1.0)(1.3)} = 0.77V_e \quad (5)$$

$$\frac{V_e}{R_d R_o} \gamma_{95th} = \frac{V_e}{(2.0)(1.5)} \gamma_{95th} = 0.33 \gamma_{95th} V_e \quad (6)$$

$$\gamma_{95th} \geq \frac{0.77 V_e}{0.33 V_e} = 2.31 \quad (7)$$

5 – CONCLUSION

This paper investigated various approaches to obtain the overstrength factor values for multi-panel CLT shear walls based on the panel-to-panel connections. The main conclusions are:

1. A ratio of the 95th to 5th percentiles equal to 1.3 for the tested connections seems reasonable regardless of displacement level.
2. The discrepancy between the design capacity and the 5th percentile of the cyclic test results significantly affects the overstrength factor values, resulting in the analytical overstrength factor being very conservative based on the design capacity obtained from the Canadian timber design standard. In several cases the total over-strength factor exceeds the value associated with elastic design. An approach for selecting an appropriate displacement level to calculate the overstrength factor is needed.

6 – REFERENCES

- [1] CSA, 2024, *CSA O86:24 Engineering Design in Wood*, CSA O86:19, Canadian Standards Association (CSA) Group, Mississauga, ON.
- [2] Yuxin Pan, Thomas Teflissi, and Thomas Tannert, 2024, “Experimental Parameter Study on CLT Shear Walls with Self-Tapping Screw Connections,” *Journal of Structural Engineering*, **150**(1). <https://doi.org/10.1061/jsendh.steng-12710>.
- [3] Masroor, M., Doudak, G., and Casagrande, D., 2022, “Design of Multipanel CLT Shear Walls with Bidirectional Mechanical Anchors Following Capacity-Based Design Principle,” *J. Perform. Constr. Facil.*, **36**(1). [https://doi.org/10.1061/\(ASCE\)CF.1943-5509.0001693](https://doi.org/10.1061/(ASCE)CF.1943-5509.0001693).
- [4] Taylor, B., Barbosa, A. R., and Sinha, A., 2020, “Cyclic Performance of In-Plane Shear Cross-Laminated Timber Panel-to-Panel Surface Spline Connections,” *Eng. Struct.*, **218**, p. 110726. <https://doi.org/10.1016/j.engstruct.2020.110726>.
- [5] Gavric, I., Fragiaco, M., and Ceccotti, A., 2015, “Cyclic Behavior of CLT Wall Systems: Experimental Tests and Analytical Prediction Models,” *J. Struct. Eng. N. Y. N.*, **141**(11). [https://doi.org/10.1061/\(ASCE\)ST.1943-541X.0001246](https://doi.org/10.1061/(ASCE)ST.1943-541X.0001246).
- [6] Casagrande, D., Rossi, S., Sartori, T., and Tomasi, R., 2016, “Proposal of an Analytical Procedure and a Simplified Numerical Model for Elastic Response of Single-Storey Timber Shear-Walls,” *Constr Build Mater*, **102**, pp. 1101–1112.
- [7] Hristovski, V., Mircevski, V., Dujic, B., and Garevski, M., 2018, “Comparative Dynamic Investigation of Cross-Laminated Wooden Panel Systems: Shaking-Table Tests and Analysis,” *Adv. Struct. Eng.*, **21**(10), pp. 1421–1436. <https://doi.org/10.1177/1369433217749766>.
- [8] Flatscher, G., and Schickhofer, G., 2015, “Shaking-Table Test of a Cross-Laminated Timber Structure,” *Proc. Inst. Civ. Eng. - Struct. Build.*, **168**(11), pp. 878–888. <https://doi.org/10.1680/stbu.13.00086>.
- [9] Ceccotti, A., and Follesa, M., 2006, “Seismic Behaviour of Multi-Storey XLam Buildings.”
- [10] Dujic, B., Aicher, S., and Zarnič, R., 2005, “Investigations on In-Plane Loaded Wooden Elements – Influence of Loading and Boundary Conditions,” *Otto-Graf-J.*, **16**, pp. 259–272.
- [11] Dujic, B., Pirmanšek, K., Zarnič, R., and Ceccotti, A., 2010, “PREDICTION OF DYNAMIC RESPONSE OF A 7-STORY MASSIVE XLAM WOODEN BUILDING TESTED ON A SHAKING TABLE.”
- [12] Ceccotti, A., Follesa, M., Lauriola, M. P., and Sandhaas, C., 2006, “SOFIE PROJECT - TEST RESULTS ON THE LATERAL RESISTANCE OF CROSS-LAMINATED WOODEN PANELS,” *First European Conference on Earthquake Engineering and Seismology*, Geneva, Switzerland.
- [13] Popovski, M., Schneider, J., and Schweinsteiger, M., 2010, “Lateral Load Resistance of Cross-Laminated Wood Panels.”
- [14] Yasumura, M., Kobayashi, K., Okabe, M., Miyake, T., and Matsumoto, K., 2016, “Full-Scale Tests and Numerical Analysis of Low-Rise CLT Structures under Lateral Loading,” *J. Struct. Eng. N. Y. N.*, **142**(4). [https://doi.org/10.1061/\(ASCE\)ST.1943-541X.0001348](https://doi.org/10.1061/(ASCE)ST.1943-541X.0001348).
- [15] Popovski, M., and Gavric, I., 2016, “Performance of a 2-Story CLT House Subjected to Lateral Loads,” *J. Struct. Eng.*, **142**(4), p. E4015006. [https://doi.org/10.1061/\(ASCE\)ST.1943-541X.0001315](https://doi.org/10.1061/(ASCE)ST.1943-541X.0001315).

- [16] Hummel, J., Flatscher, G., Schickhofer, G., and Seim, W., 2013, *CLT Wall Elements under Cyclic Loading - Details for Anchorage and Connection*.
- [17] Masroor, M., Doudak, G., and Casagrande, D., 2024, "Validation of Proposed Analytical Model and Design Procedures for Multi-Panel CLT Shearwalls Through Experimental Investigation," *Proceedings of the Canadian Society of Civil Engineering Annual Conference 2022*, R. Gupta, M. Sun, S. Brzev, M.S. Alam, K.T.W. Ng, J. Li, A. El Damatty, and C. Lim, eds., Springer Nature Switzerland, pp. 27–43. https://doi.org/10.1007/978-3-031-34027-7_3.
- [18] Joyce, T., Ballerini, M., and Smith, I., 2011, "Mechanical Behaviour of In-Plane Shear Connections between CLT Wall Panels," Alghero, Italy.
- [19] Gavric, I., Fragiaco, M., and Ceccotti, A., 2015, "Cyclic Behavior of Typical Screwed Connections for Cross-Laminated (CLT) Structures," *Eur. J. Wood Wood Prod.*, **73**(2), pp. 179–191. <https://doi.org/10.1007/s00107-014-0877-6>.
- [20] Gavric, I., Fragiaco, M., and Ceccotti, A., 2014, "Cyclic Behaviour of Typical Metal Connectors for Cross-Laminated (CLT) Structures," *Mater. Struct.*, **48**(6), pp. 1841–1857. <https://doi.org/10.1617/s11527-014-0278-7>.
- [21] Sullivan, K., Miller, T. H., and Gupta, R., 2018, "Behavior of Cross-Laminated Timber Diaphragm Connections with Self-Tapping Screws," *Eng. Struct.*, **168**, pp. 505–524. <https://doi.org/10.1016/j.engstruct.2018.04.094>.
- [22] Hossain, A., Danzig, I., and Tannert, T., 2016, "Cross-Laminated Timber Shear Connections with Double-Angled Self-Tapping Screw Assemblies," *J. Struct. Eng. N. Y. N.*, **142**(11). [https://doi.org/10.1061/\(ASCE\)ST.1943-541X.0001572](https://doi.org/10.1061/(ASCE)ST.1943-541X.0001572).
- [23] Casagrande, D., Polastri, A., Sartori, T., and Loss, C., 2016, "Experimental Campaign for the Mechanical Characterization of Connection Systems in the Seismic Design of Timber Buildings," Vienna, Austria. [Online]. Available: <https://research.thinkwood.com/en/permalink/catalogue1511>.
- [24] Hossain, A., Popovski, M., and Tannert, T., 2019, "Group Effects for Shear Connections with Self-Tapping Screws in CLT," *J. Struct. Eng. N. Y. N.*, **145**(8). [https://doi.org/10.1061/\(ASCE\)ST.1943-541X.0002357](https://doi.org/10.1061/(ASCE)ST.1943-541X.0002357).
- [25] Jorissen, A. J. M., and Fragiaco, M., 2011, "General Notes on Ductility in Timber Structures," *Eng. Struct.*, **33**(11), pp. 2987–2997. <https://doi.org/10.1016/j.engstruct.2011.07.024>.
- [26] ASTM, 2022, "Standard Practice for Sampling and Data-Analysis for Structural Wood and Wood-Based Products, ASTM D2915-17." <https://doi.org/10.1520/D2915-17R22>.
- [27] ASTM, 2019, "Standard Test Methods for Cyclic (Reversed) Load Test for Shear Resistance of Vertical Elements of the Lateral Force Resisting Systems for Buildings, ASTM E2126-19." <https://doi.org/10.1520/E2126-19>.
- [28] ISO, 2019, "Timber Structures — Joints Made with Mechanical Fasteners — Quasi-Static Reversed-Cyclic Test Method, ISO 16670:2003."
- [29] CEN, 2001, "Timber Structures - Test Methods - Cyclic Testing of Joints Made with Mechanical Fasteners EN 12512."
- [30] Link, C. L., 1985, *An Equation for One-Sided Tolerance Limits for Normal Distributions*, FPL 458, U.S. Department of Agriculture, Forest Service, Forest Products Laboratory, Madison, WI.
- [31] CEN, 1991, "Timber Structures - Joints Made with Mechanical Fasteners - General Principles for the Determination of Strength and Deformation Characteristics EN26891."
- [32] Canadian Commission on Building and Fire Codes, 2022, *National Building Code of Canada: 2020*, 978-0-660-37913-5, National Research Council of Canada. <https://doi.org/10.4224/w324-hv93>.